

Supporting Information for

Facile Synthesis of Rhombic Dodecahedral AgX/Ag₃PO₄ (X=Cl, Br, I)

Hetero-crystals with Enhanced Photocatalytic Properties and Stabilities

Yingpu Bi, Shuxin Ouyang, Junyu Cao, and Jinhua Ye *

*International Center for Materials Nanoarchitectonics (MANA), and Photocatalytic Materials Center,
National Institute for Materials Science (NIMS), 1-2-1 Sengen, Tsukuba, Ibaraki 305-0047, Japan*

*To whom correspondence should be addressed.

Email: jinhua.ye@nims.go.jp

Experimental Section

1. Synthesis of rhombic dodecahedral Ag₃PO₄ crystals

The rhombic dodecahedral Ag₃PO₄ crystals were prepared by a simple precipitation process. In a typical synthesis, CH₃COOAg (0.5 g) was solved in aqueous solution containing poly (vinyl pyrrolidone) (PVP, $M_w \approx 50000$, 150 mM as calculated in terms of the repeating unit). NaH₂PO₄ aqueous solution (0.15 M) was added with drop by drop to the above solution. The resulting mixture was maintained at room temperature for 8 h until its colour became golden yellow. The obtained samples for morphology and structure analysis were washed with water to remove the CH₃COO⁻ and PVP and dried under atmosphere.

2. Synthesis of rhombic dodecahedral AgX/Ag₃PO₄ hetero-crystals

The obtained Ag₃PO₄ rhombic dodecahedral crystals were further reacted with appropriate sodium halide solutions (0.2 M) including NaCl, NaBr, and NaI, in which these special shaped Ag₃PO₄ crystals were used as both template and silver ion source. During this ions-exchange process, the Ag₃PO₄ on the surfaces of the rhombic dodecahedral crystals could be readily replaced by halide ions to form AgX nanofilms, thereby the AgX/Ag₃PO₄ core-shell heterocrystals with rhombic dodecahedral structure have been synthesized.

3. Photocatalytic Reactions

In all catalytic activity of experiments, the samples (0.2 g) were put into a solution of MO dye (100 ml, 40 mg/L,), which was then irradiated with a 300W Xe arc lamp equipped with an ultraviolet cutoff filter to provide visible light with $\lambda \geq 420$ nm. The degradation of MO dye was monitored by UV/Vis spectroscopy (UV-2500PC, Shimadzu). Before the spectroscopy measurement, these photocatalysts were removed from the photocatalytic reaction systems by a dialyzer.

4. Photoelectric Conversions

The photoelectric conversion properties were investigated in a conventional three-electrode cell by using computer-controlled electrochemical workstation (CHI 650A). 50 mg catalysts was suspended in 2 mL nafion aqueous solution (1 wt%), the mixtures were ultrasonically scattered for 15 min to form homogeneous solution. Then, 0.1 mL solution was dropped on the Fluorine doped tin oxide (FTO) glass (0.5×4 cm). After evaporation of the water in air, the catalysts was attached onto the surface of FTO glass. A Pt wire, saturated calomel electrode (SCE), and 0.1 M sodium sulfate were used as the working electrode, the counter-electrode, the reference electrode, and the electrolyte, respectively. The current-time (*i-t*) curves were collected at 1 V vs SCE. The light source was a 300W Xe lamp, and a cutoff filter of 420nm was employed for the visible-light irradiation.

5. Characterizations

SEM and FE-SEM images were taken using a field-emission scanning electron microscope (JSM-6701F, JEOL) operated at an accelerating voltage of 5 kV. An energy-dispersive (ED) detector was equipped with this field-emission scanning electron microscope and operated at an accelerating voltage of 15 kV. The X-ray diffraction spectra (XRD) measurements were performed on a Philips X' pert MPD instrument using Cu K α radiation (50 kv). The XRD patterns were recorded from 10° to 90° with a scanning rate of 0.067°/ s. The infrared spectra were obtained on a Fourier Transform Infrared (FTIR) Spectrometer (Shimadzu IRprestige-21). UV/Vis absorption spectra were taken at room temperature on a UV-2550 (Shimadzu) spectrometer.

Additional Figures

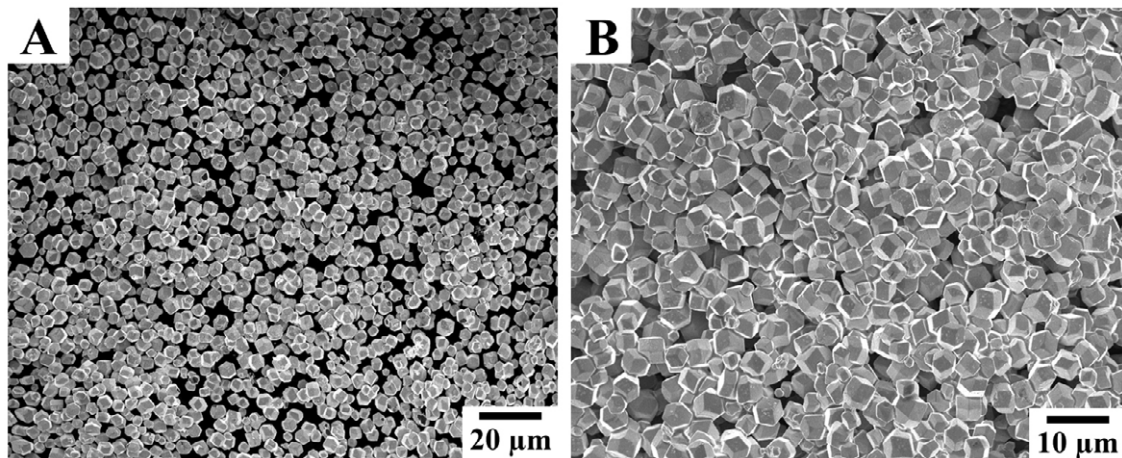


Fig. S1. (A-B) SEM images of rhombic dodecahedral Ag_3PO_4 crystals with different magnifications.

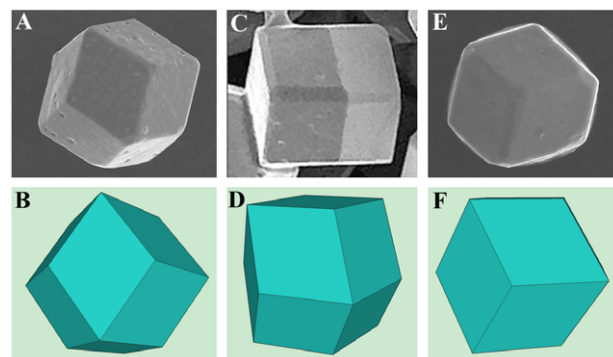


Fig. S2. SEM images of as-prepared Ag_3PO_4 crystals (A, C, E) and geometrical models of ideal rhombic dodecahedrons with different view angles (B, D, F).

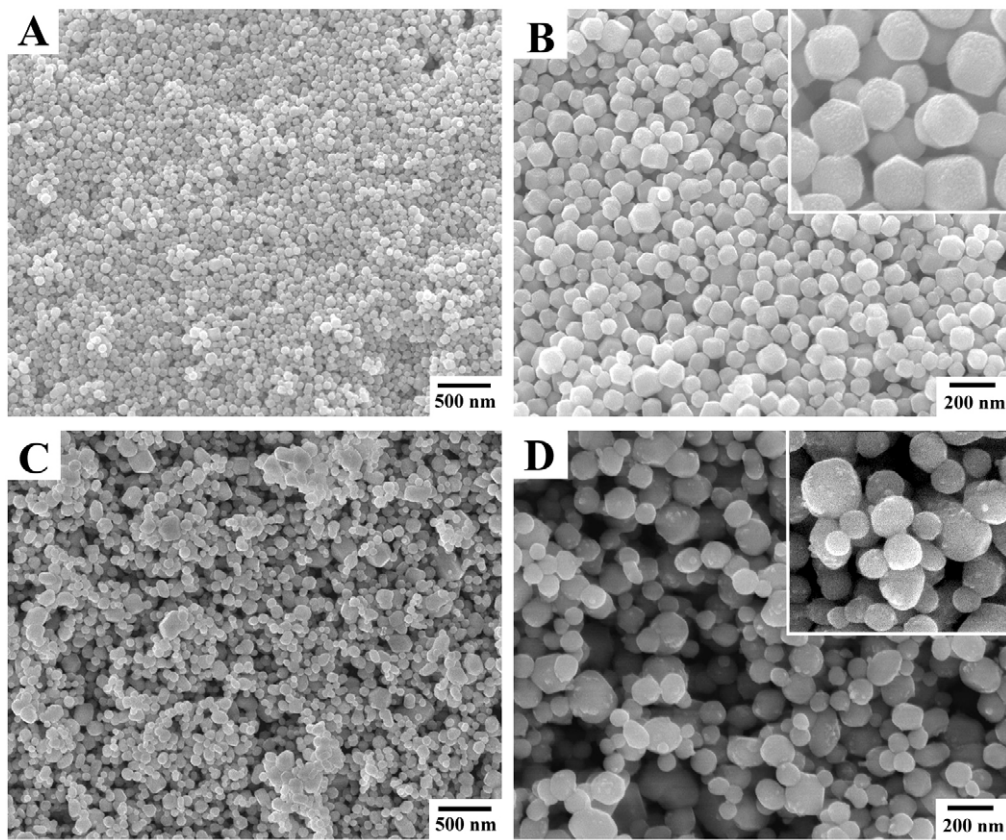


Fig. S3. (A-B) SEM images of rhombic dodecahedral Ag_3PO_4 crystals with increasing the PVP concentrations to 500 mM; (C-D) SEM images of Ag_3PO_4 crystals prepared by using AgNO_3 as precursor.

Additional discussions

Furthermore, it should be noted that the PVP and silver precursor play important roles in determining the dimensions, structure, and morphologies of the as-prepared Ag_3PO_4 products. As shown in Figure A and B, when PVP concentration was increased up to 500 mM, the dimensions of rhombic dodecahedral Ag_3PO_4 nanoproducts were reduced to 100 nm, and no obvious structural change has been observed. On the other hand, when CH_3OOAg was replaced by AgNO_3 , the synthesized Ag_3PO_4 products possess large dimensions and irregular structures. Thereby, we speculate that in the present synthetic system, the CH_3OO^- ions may selectively absorbed on the various crystal planes of the Ag_3PO_4 crystals, which induces their anisotropic growth into rhombic dodecahedral structures.

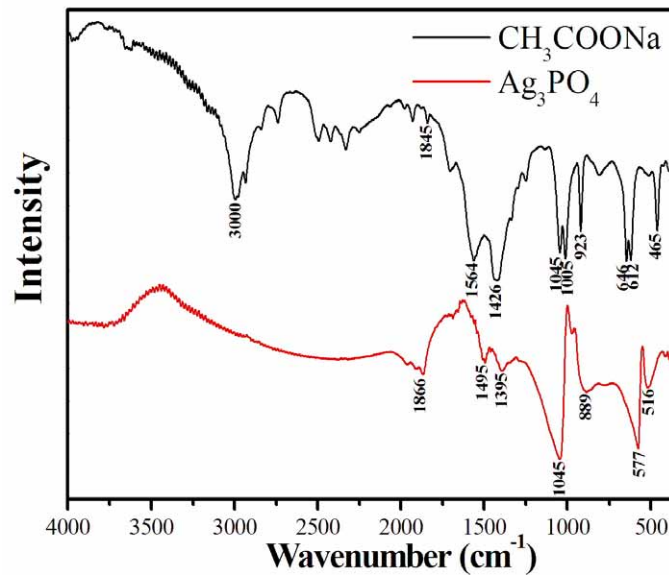


Fig. S4. FTIR spectra of CH₃COONa and as-prepared rhombic dodecahedral Ag₃PO₄ crystals.

FTIR analysis of the as-prepared Ag₃PO₄ crystals

The infrared spectra of both CH₃COONa and rhombic dodecahedral Ag₃PO₄ crystals have been both shown in Figure S4. It can be clearly seen that pure CH₃COONa displays the characteristic absorption peaks of the asymmetric and symmetric stretching vibrations of COO bands at 1564 and 1426 cm⁻¹, respectively.^{1,2} Furthermore, the infrared spectrum of rhombic dodecahedral Ag₃PO₄ crystals is nearly identical to that of CH₃COONa spectra although the absorption peaks intensities and positions have been slightly shifted. More specifically, the symmetric and asymmetric absorption peaks of COO bands have been both shifted to 1495 and 1395 cm⁻¹ over rhombic dodecahedral Ag₃PO₄ crystals, indicating that there is weak chemical bonding of COO to Ag₃PO₄ at the interface between CH₃COO⁻ and the crystals. These observations clearly confirm that CH₃COO⁻ molecule could adsorb onto the surfaces of Ag₃PO₄ crystals, which may selectively control their various crystal planes growth.

Reference

1. M. Saboktakin, A. Maharramov, M. Ramazanov, *J. Am. Sci.* **2007**, 3, 30.
2. H. Ichiura, Y. Kaneda, Y. Ohtani, *J. Mater. Sci.* **2010**, 45, 1343.

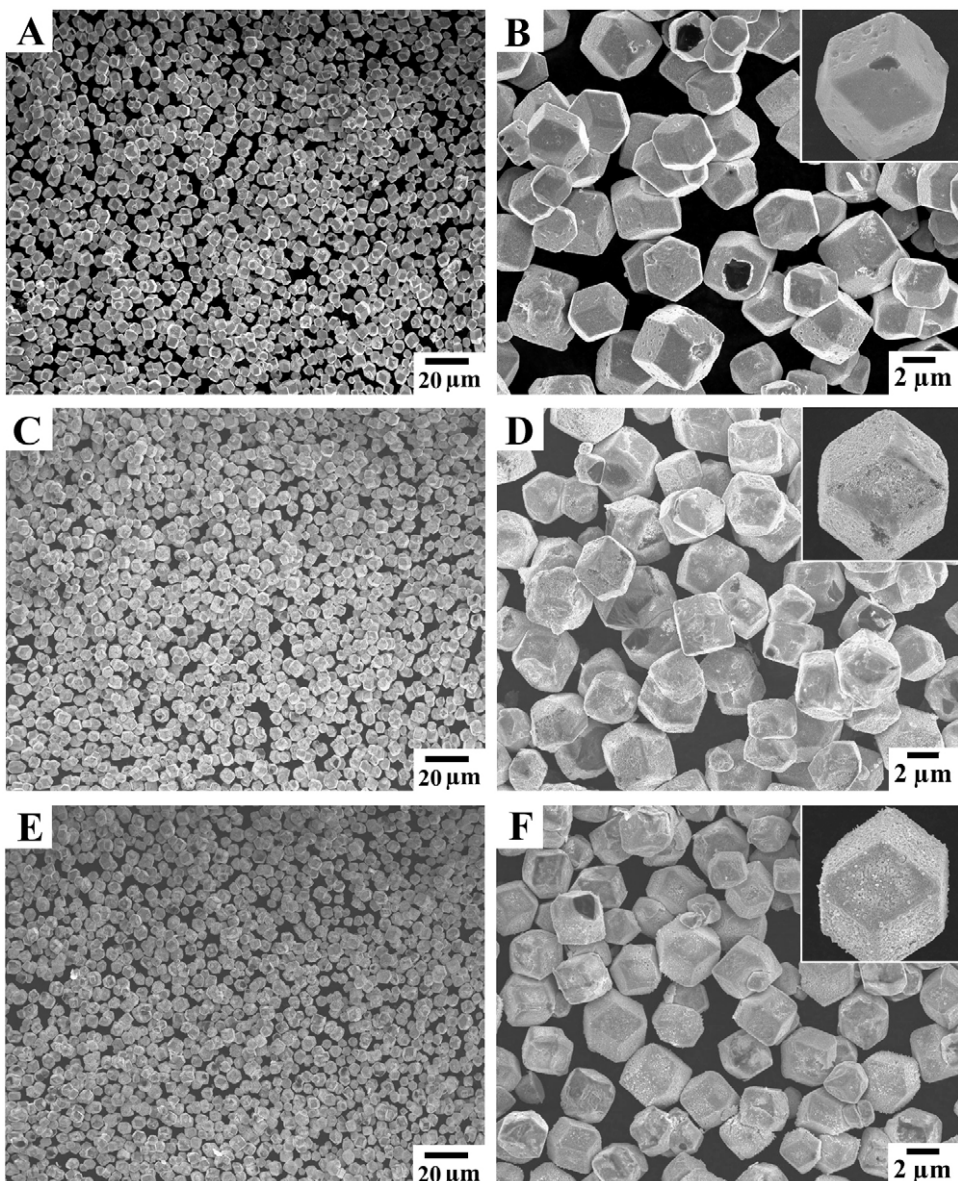


Fig. S5. (A-B) SEM images of rhombic dodecahedral AgCl/Ag₃PO₄ hetero-crystals; (C-D) SEM images of rhombic dodecahedral AgBr/Ag₃PO₄ hetero-crystals; (E-F) SEM images of rhombic dodecahedral AgI/Ag₃PO₄ hetero-crystals.

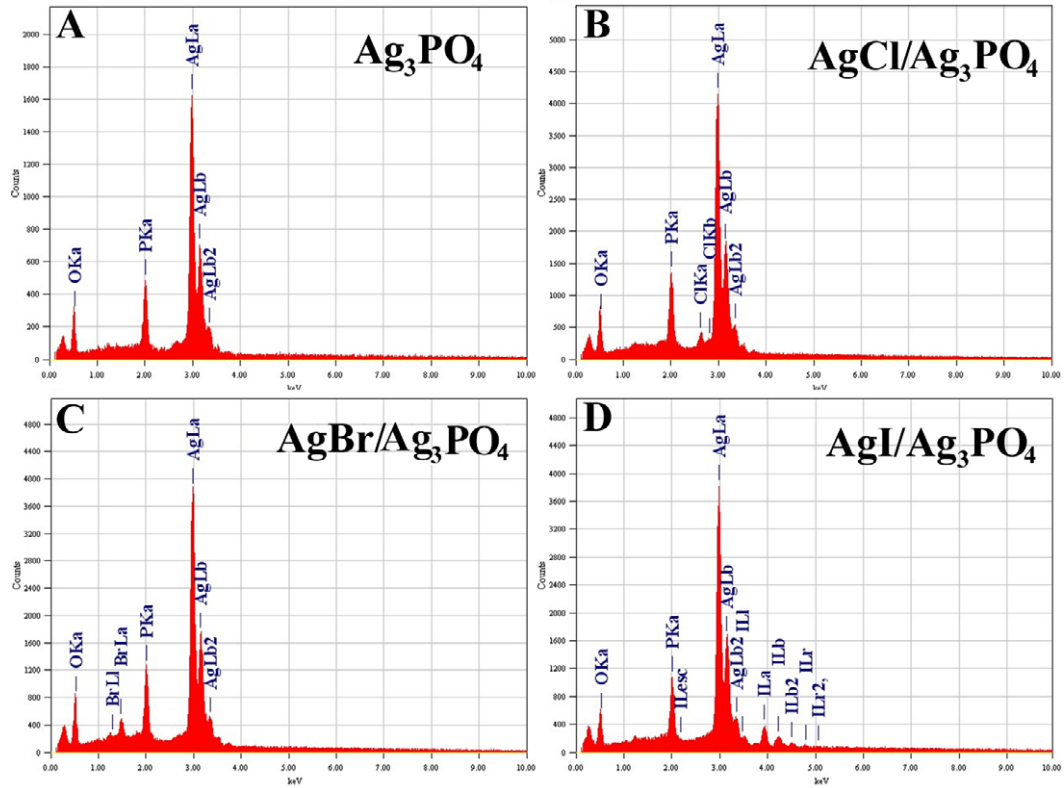


Fig. S6. (A) EDS pattern of rhombic dodecahedral Ag_3PO_4 crystals; (B) EDS pattern of rhombic dodecahedral $\text{AgCl}/\text{Ag}_3\text{PO}_4$ hetero-crystals; (C) EDS pattern of rhombic dodecahedral $\text{AgBr}/\text{Ag}_3\text{PO}_4$ hetero-crystals; (D) EDS pattern of rhombic dodecahedral $\text{AgI}/\text{Ag}_3\text{PO}_4$ hetero-crystals.

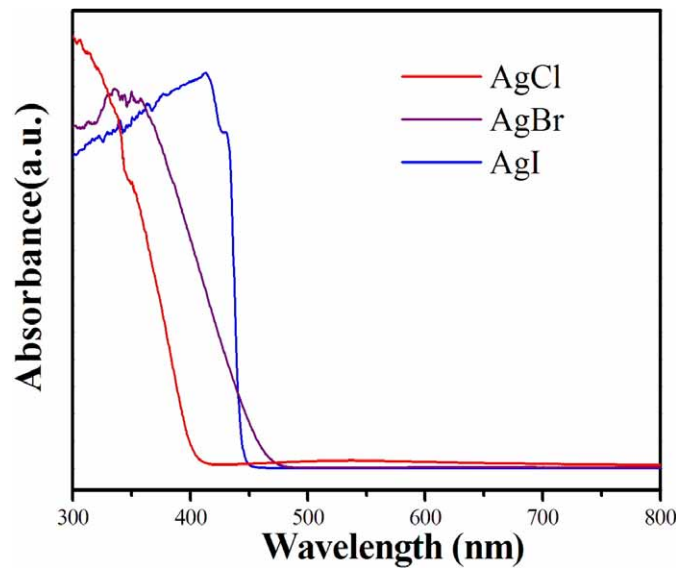


Fig. S7. Ultraviolet–visible diffusive reflectance spectrum of the pure AgCl, AgBr, and AgI samples.

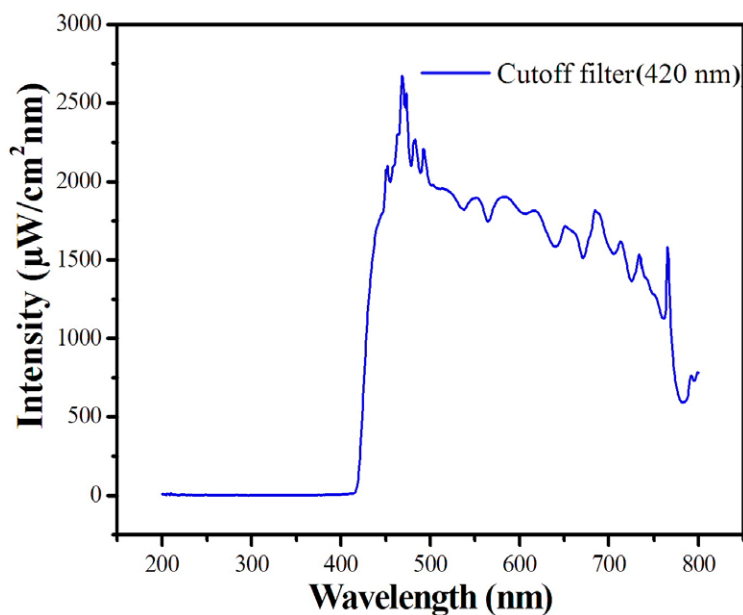


Fig. S8. The intensity and wavelength distribution of the irradiation light employed in the organic decomposition experiments. Integral intensities were measured under the actual experimental conditions.

Table S1. BET (Brunauer–Emmer–Teller) surface area and pH values of Ag_3PO_4 and $\text{AgX}/\text{Ag}_3\text{PO}_4$

	Ag_3PO_4	$\text{AgCl}/\text{Ag}_3\text{PO}_4$	$\text{AgBr}/\text{Ag}_3\text{PO}_4$	$\text{AgI}/\text{Ag}_3\text{PO}_4$
Surface area (m^2/g)	0.17	0.32	0.19	0.25
pH value	8.02	7.28	7.43	7.16

BET (Brunauer–Emmer–Teller) surface area and pH values

Furthermore, the BET (Brunauer–Emmer–Teller) surface area of these catalysts and their pH values in aqueous solution have been both measured and shown in the Table S1. It can be clearly seen that the surface areas of as-prepared $\text{AgX}/\text{Ag}_3\text{PO}_4$ hetero-crystals are all larger than that of Ag_3PO_4 crystals, which may partially contribute to their higher photocatalytic activities. Moreover, after epitaxial growth of AgX nanolayers, the pH values of as-prepared $\text{AgX}/\text{Ag}_3\text{PO}_4$ hetero-crystals in aqueous solution are all lower than that of Ag_3PO_4 crystals, which may facilitate the adsorption of the negatively charged MO ions onto the surfaces of photocatalysts owing to the coulombic attractive force^{1,2}.

Reference

1. S. Al-Qaradawi, S. Salman, *J. Photoch. Photobio. A*, 2002, 148, 161.
2. S. Kansal, M. Singh, D. Sud, *J. Hazard. Mater.*, 2007, 141, 581.

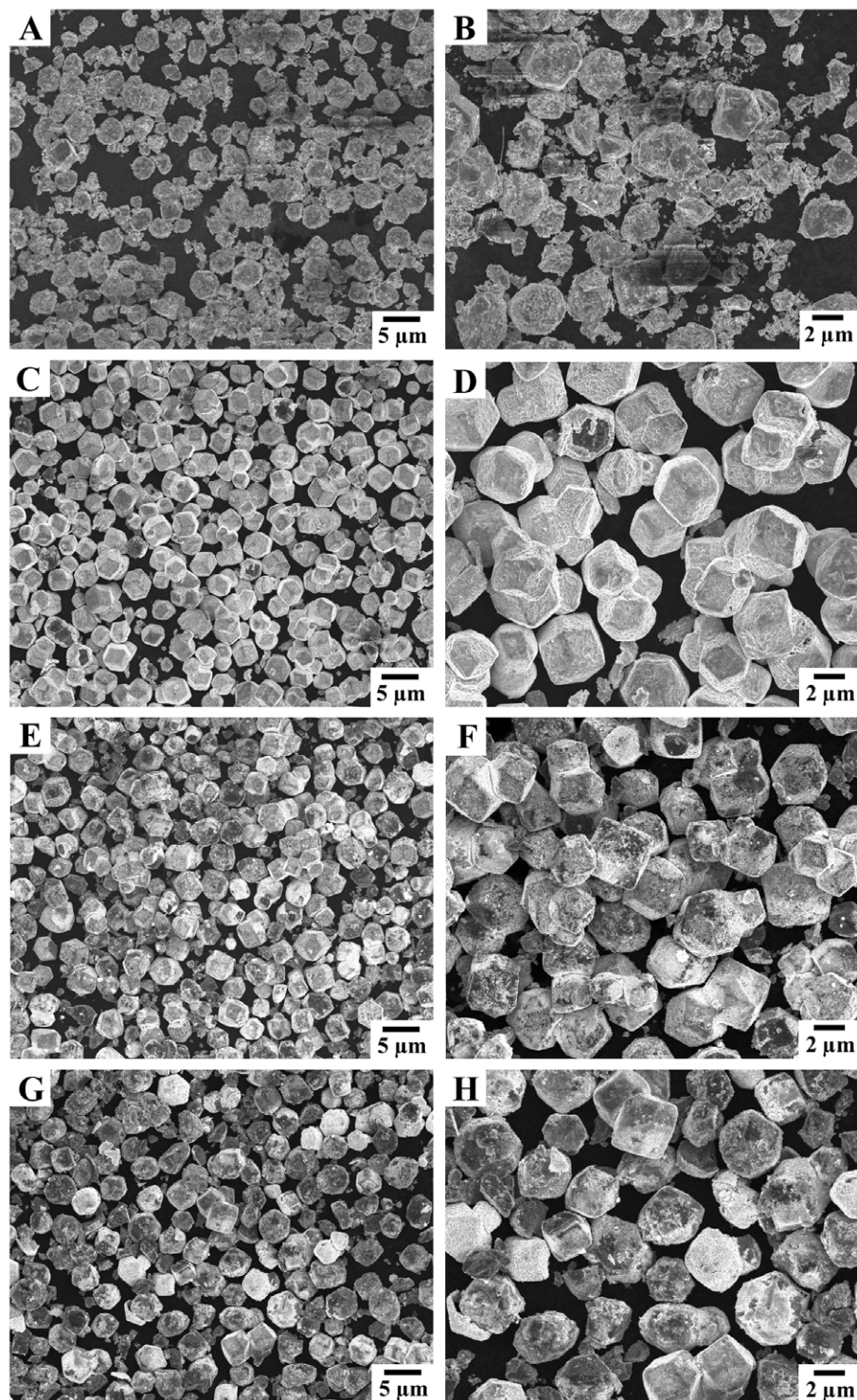


Fig. S9. SEM images of (A-B) Ag₃PO₄, (C-D) AgCl/Ag₃PO₄, (E-F) AgBr/Ag₃PO₄, and (G-H) AgI/Ag₃PO₄ catalysts after MO decomposition experiments.

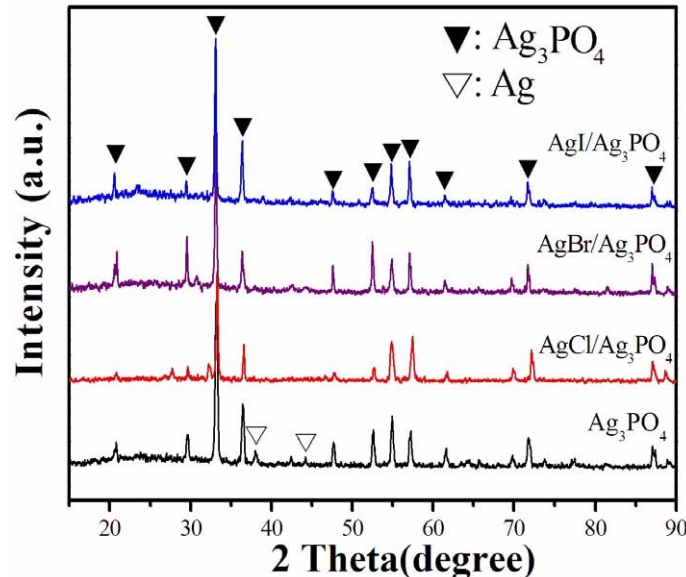


Fig. S10. XRD patterns of Ag_3PO_4 , $\text{AgCl}/\text{Ag}_3\text{PO}_4$, $\text{AgBr}/\text{Ag}_3\text{PO}_4$, and $\text{AgI}/\text{Ag}_3\text{PO}_4$ catalysts after MO decomposition experiments.

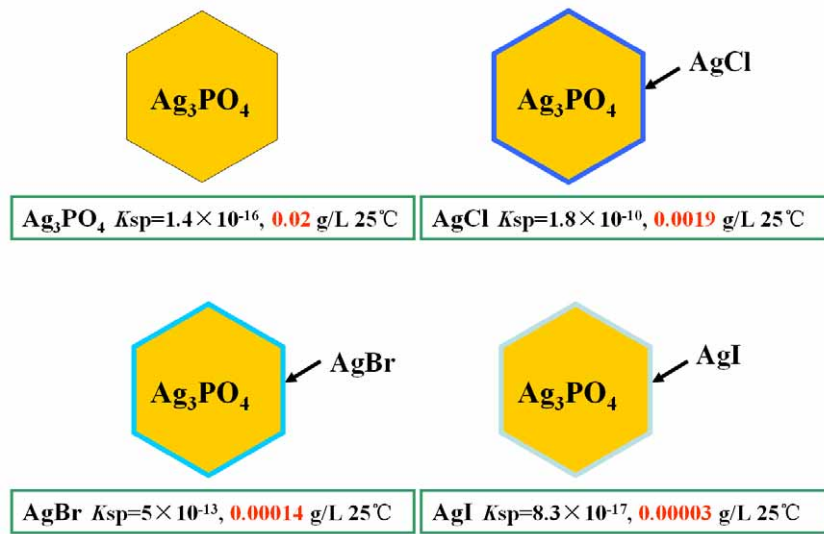


Fig. S11. The scheme of Ag_3PO_4 and $\text{AgX}/\text{Ag}_3\text{PO}_4$ hetero-crystals with different solubility and K_{sp} .